Dislocation Patterning: From Micro- to Mesoscale Description

I. Groma and B. Bakó

Eötvös University, Department of General Physics, P.O. Box 32, 1518 Budapest, Hungary

(Received 4 August 1999)

During the plastic deformation of crystalline material the dislocations, being the carriers of the plastic flow, tend to form different patterns. Because of the long range nature of dislocation-dislocation interaction, the origin of this self-ordering phenomenon is still an open question. The paper presents a stochastic two-dimensional model derived directly from the properties of individual dislocations making it possible to investigate the problem on a mesoscale. Numerical results obtained in double slip configuration indicate the development of cell structure with fractal character.

PACS numbers: 61.72.Lk, 61.72.Bb, 61.72.Cc

It is well known that during the plastic deformation of crystalline materials dislocations form different structures. Although a huge amount of experimental and theoretical work has been done over the past three decades, there is not a generally accepted model for dislocation patterning. Since the time evolution of the dislocation network is an extremely complex process, the goal of the analytical and numerical investigations is to find out the important dislocation phenomena responsible for the development of ordered dislocation networks.

Several analytical models (the concept of low energy dislocation structure proposed by Kulhman-Wilsdorf [1], the models of Holt [2] and Rickman and Viñals [3] that apply irreversible thermodynamics analogy, the reaction-diffusion approach elaborated by Walgraef and Aifantis [4], the concept of the dislocation sweeping mechanism developed by Kratochvil *et al.* [5,6], and the stochastic dislocation dynamics description proposed by Hähner [7]) have been developed since dislocation patterning was first observed. The common feature of these models is that the behavior of the dislocation system is described on a continuum level by operating with balance equations of different densities. Most of them are based on analogy with other physical problems such as spinodal decomposition, oscillating chemical reactions, etc. As a consequence of this, the properties of individual dislocations are taken into account only in a very indirect way, making questionable the validity of the models proposed thus far.

Another possible approach to study the collective behavior of dislocations is the numerical integration of the equations of motion of dislocations. Several investigations have been performed both in 2D [8–17] and in 3D [18,19]. Most of them predict tendency of formation of organized dislocation structures but they are far from convincing. This is mainly due to the fact that because of the long range dislocation-dislocation interaction the numerical integration of the equations of motion of dislocations is computationally very expensive, limiting considerably the affordable size of simulation volume and dislocation density.

The aim of the present paper is to outline a method which is able to deal with a mesoscopic size dislocation assembly and in which the precise form of dislocation-dislocation interaction is directly taken into account. It is important to stress that the proposed mesoscale evolution equations are derived from the equations of motion of the individual dislocations, so the mesoscale and the microscale are directly linked. For reducing the complexity only the time evolution of a system of parallel straight edge dislocations (with line vector $\mathbf{l}$) is considered resulting a 2D problem, but it seems to be feasible to extend the model to more realistic 3D configurations.

In order to derive the governing equations on mesoscale let us start with the dynamics of interacting individual edge dislocations. Because of the dissipative nature of the dislocation motion, in the equation of motion of a dislocation a friction force has to be taken into account beside the force acting on a dislocation due to the elastic field [the Peach-Koehler (PK) force]. The friction force is commonly (almost in each numerical simulation known by the authors) assumed to be proportional to the dislocation velocity. (It describes friction related to phonon creation.) Since in most cases the inertia term is negligible compared to the PK force, the dynamics of the dislocations can be described with an over-damped-type system of equations of motion [13], i.e., for the kth dislocation,

$$\mathbf{v}_k = B\mathbf{F}_s^k = B[\mathbf{b}_k(\sigma_0 + \sigma_{\text{int}})\mathbf{n}_k]\mathbf{b}_k/|\mathbf{b}_k|, \qquad k = \overline{1,N}, \tag{1}$$

where $\mathbf{b}_k$ is the Burgers vector of the kth dislocation, $\mathbf{n}_k = \mathbf{b}/|\mathbf{b}| \times \mathbf{k}$ is a unit vector perpendicular to $\mathbf{b}_k$, σ_{int} is the stress tensor field created by the entire dislocation system, σ_0 is the external stress tensor, and B is the dislocation mobility. As it is explained in [20], the internal force (the projection of the PK force to the slip plane) $\mathbf{F}_k^{\text{int}} = [\mathbf{b}_k\sigma_{\text{int}}\mathbf{n}_k]\mathbf{b}_k/|\mathbf{b}_k|$ can be derived from a potential, $\mathbf{F}_k^{\text{int}} = -\mathbf{b}_k/|\mathbf{b}_k|\,(\mathbf{b}_k\nabla)V_k$, where V_k is given by the expression

$$V_k(\mathbf{r}) = -\frac{(\mathbf{n}_k\nabla)}{b_k}\sum_{j\neq k}^{N}(\mathbf{n}_j\nabla)g(\mathbf{r}-\mathbf{r}^j), \qquad g(\mathbf{r}) = \frac{r^2}{2}\ln(r). \tag{2}$$

In most of the two-dimensional dislocation dynamics simulations Eq. (1) is integrated numerically. Because of

the long range nature of dislocation-dislocation interaction, however, studying the long time behavior of a dislocation assembly is extremely computation expensive within the level of this "discrete" dislocation description. For single glide it was shown by Groma [21,22] that if short range correlations are negligible, i.e., the system is not far from homogeneous, a self-consistent field (SCF)-type continuum approach can be derived from Eq. (1). The SCF model can be generalized for a configuration of n_s slip systems (in the 2D configuration considered, this means that dislocations with more than one type of Burgers vectors $\mathbf{b}_l, l = \overline{1, n_s}$ are introduced into the system) by carrying out the following steps: the equation of motion of the ith dislocation (1) is multiplied by the delta function $\delta(\mathbf{r} - \mathbf{r}_k)$ and differentiated with respect to $\mathbf{r}$, then the equations are summed up separately for dislocations with different Burgers vectors, resulting $2n_s$ relations for the $\sum_k \delta(\mathbf{r} - \mathbf{r}_k)$-type discrete dislocation densities. Finally, the discrete densities are replaced by locally averaged ("smoothed") densities. It can be shown [21] that this last step can be done only if short range correlations are negligible.

Let us denote by $\rho_{\pm}^{l}(\mathbf{r}, t)$ the smoothed density functions of dislocations with Burgers vector $\pm\mathbf{b}_l$, and introduce the notations $\rho_l(\mathbf{r}) = \rho_+^l(\mathbf{r}) + \rho_-^l(\mathbf{r})$, and $k_l(\mathbf{r}) = \rho_+^l(\mathbf{r}) - \rho_-^l(\mathbf{r})$ for the l-type "total," and "sign" dislocation densities, respectively. With these, in the SCF approximation the potential V_l defined above has the form

$$V_l(\mathbf{r}) = -\frac{(\mathbf{n}_l\nabla)}{b_l} \sum_{j=1}^{n_s} (\mathbf{n}_j\nabla)\,(k_j \star g)\,, \tag{3}$$

where $k_j \star g = \int k_j(\mathbf{r}')g(\mathbf{r} - \mathbf{r}')\,d\mathbf{r}'$. The time evolution of the dislocation system is described by the following set of balance equations:

$$\frac{\partial\rho_l(\mathbf{r}, t)}{\partial t} B(\mathbf{b}_l\nabla)k_l(\mathbf{r}, t)\left[\tau_l - \frac{(\mathbf{b}_l\nabla)}{b_l} V_l(\mathbf{r})\right] = 0\,, \tag{4}$$

$$\frac{\partial k_l(\mathbf{r}, t)}{\partial t} B(\mathbf{b}_l\nabla)\rho_l(\mathbf{r}, t)\left[\tau_l - \frac{(\mathbf{b}_l\nabla)}{b_l} V_l(\mathbf{r})\right] = 0\,, \tag{5}$$

where $\tau_l = \mathbf{b}_l\sigma_0\mathbf{n}_l$ stands for the external resolved shear stress in the lth slip system. If dislocation multiplication is allowed, a source term needs to be added to the right-hand side of Eq. (4), but in the studies presented in this paper the number of dislocations has been kept constant.

It is easy to see that, if the external stress is constant, the homogeneous stationary solution $\rho_l(\mathbf{r}, t) = \rho_l^0$, $k_l(\mathbf{r}, t) = 0$ satisfies the SCF equations [Eqs. (4) and (5)]. It has to be investigated, however, whether this trivial solution is a stable one. For this, the usual technique of linear stability analysis can be applied.

Let us seek the solution of Eqs. (4) and (5) in the form $\rho_l(\mathbf{r}, t) = \overline{\rho}_l + \delta\rho_l(\mathbf{r}, t)$, $k_l(\mathbf{r}, t) = \delta k_l(\mathbf{r}, t)$, $l = \overline{1, n_s}$, where $\delta\rho_l(\mathbf{r}, t)$ and $\delta k_l(\mathbf{r}, t)$ are small perturbations, so their higher order terms can be neglected. The solution of the corresponding linearized equations can be found in the form

$$\begin{aligned} \delta\rho_l &= \delta\rho_l^0 \exp(\lambda t + i\mathbf{q}\cdot\mathbf{r})\,, \\ \delta k_l &= \delta k_l^0 \exp(\lambda t + i\mathbf{q}\cdot\mathbf{r}), \qquad l = \overline{1, n_s}\,, \end{aligned} \tag{6}$$

where i is the imaginary unit. After substituting the above expressions into the linearized form of Eqs. (4) and (5), one finds that $\delta\rho_l$ and δk_l have to fulfill the relations

$$\lambda\delta\rho_l + iB\tau_l(\mathbf{q}\cdot\mathbf{b}_l)\delta k_l = 0, \qquad l = \overline{1, n_s}\,, \tag{7}$$

$$\lambda\delta k_l + iB\tau_l(\mathbf{q}\cdot\mathbf{b}_l)\delta\rho_l + \frac{2\pi B\overline{\rho}_l}{bq^4}(\mathbf{q}\cdot\mathbf{b}_l)^2(\mathbf{q}\cdot\mathbf{n}_l)\sum_{j=1}^{n_s}(\mathbf{q}\cdot\mathbf{n}_j)\delta k_j = 0\,. \tag{8}$$

For single glide configuration ($n_s = 1$) it was obtained earlier [21] that, if the wave number vector $\mathbf{q}$ is either perpendicular or parallel to the Burgers vector, the real parts of the eigenvalues $\lambda_{1,2}$ are zero, meaning that these perturbations neither grow nor die out; they are stable. From Eqs. (7) and (8) for $n_s = 2$ the eigenvalues λ need to satisfy the relation

$$\lambda^4 + \frac{2\pi B\overline{\rho}_1}{bq^4}\left[(\mathbf{q}\cdot\mathbf{b}_1)^2(\mathbf{q}\cdot\mathbf{n}_1)^2 + \alpha(\mathbf{q}\cdot\mathbf{b}_2)^2(\mathbf{q}\cdot\mathbf{n}_2)^2\right]\lambda^3 + B^2\tau_1^2\left[(\mathbf{q}\cdot\mathbf{b}_1)^2 + \beta(\mathbf{q}\cdot\mathbf{b}_2)^2\right]\lambda^2 + \frac{2\pi B^3\overline{\rho}_1}{bq^4}(\mathbf{q}\cdot\mathbf{b}_1)^2(\mathbf{q}\cdot\mathbf{b}_2)^2\tau_1^2\left[\beta(\mathbf{q}\cdot\mathbf{n}_1)^2 + \alpha(\mathbf{q}\cdot\mathbf{n}_2)^2\right]\lambda + \beta B^4\tau_1^4(\mathbf{q}\cdot\mathbf{b}_1)^2(\mathbf{q}\cdot\mathbf{b}_2)^2 = 0\,, \tag{9}$$

in which the relative variables $\alpha = \overline{\rho}_2/\overline{\rho}_1$ and $\beta = (\tau_2/\tau_1)^2$ were defined. With the introduction of the notations $q^2b^2B_l = (\mathbf{q}\cdot\mathbf{b}_l)^2$, $q^2N_l = (\mathbf{q}\cdot\mathbf{n}_l)^2$, $l = 1, 2$, and with the normalizations $\lambda/(Bb\tau_1 q) \longrightarrow \lambda$ and $(\tau_1 q)/(2\pi\overline{\rho}_1) \longrightarrow q$, Eq. (9) can be simplified to

$$\lambda^4 + \frac{B_1N_1 + \alpha B_2N_2}{q}\lambda^3 + (B_1 + \beta B_2)\lambda^2 + \frac{\beta N_1 + \alpha N_2}{q}\lambda + \beta B_1B_2 = 0\,. \tag{10}$$

It can be seen from the analysis of the above form that the real part of the eigenvalues λ is never positive. It is important, however, that $\mathrm{Re}(\lambda)$ is zero for wave vectors orthogonal to the glide planes (since $B_{1,2}$ vanishes in this case), which means that perturbations propagating in these directions are preferred. Another remarkable feature of Eq. (10) is that the total dislocation density and the external stress can be scaled out, i.e., the properties in the linear regime are determined only by the relative dislocation

population α and the direction of the external stress axis (through β).

Since the SCF model neglects short range correlations (SRC), it cannot be applied in the regime where the gradients of the density fields are high. So, for investigating phenomena such as dislocation cell structure formation or development of persistent slip bands, the SCF model needs to be further developed. In order to take into account SRC a stochastic method was proposed by Bakó and Groma [23,24]. It is based on the numerical observation that the stress field generated by the dislocations has a stochastic nature. As it is explained in detail in [25], some of the features of the probability distribution function of the stress field created by the dislocations in the lth slip plane $P_l(\tau)$ can be derived analytically.

(i) The center of gravity of $P_l(\tau)$ is the self-consistent field $\tau_l^{\mathrm{SF}} = \{\tau_l - \frac{(\mathbf{b}_l \nabla)}{b_l} V_l(\mathbf{r})\}$ introduced earlier.

(ii) $P_l(\tau)$ decays asymptotically as $C\rho(\vec{r})\tau^{-3}$ (C is a constant determined by the angular anisotropy of the dislocation-dislocation interaction), i.e., the tail of the distribution function depends only on the local dislocation density.

(iii) The half width of $P_l(\tau)$ is determined by the correlation properties of the dislocation assembly.

Because of the complicated dislocation-dislocation correlations, the precise form of the stress fluctuation distribution function cannot be determined [25]. Numerical calculations show, however, that for a dislocation assembly consisting of relatively narrow dislocation dipoles the form

$$P_l(\tau) = C\rho(\mathbf{r})[(\tau - \tau_l^{\mathrm{SF}})^2(\mathbf{r}) + C\rho(\mathbf{r})]^{-3/2}, \quad (11)$$

is a good approximation of $P(\tau)$ [24].

The above results make it possible to set up the following stochastic $O(N)$ algorithm (for details, see [23]): with an appropriate coarse size the simulation area is divided into cells. Then by counting the number of different dislocations in each cell the values of the smoothed parameters $\rho_l(\mathbf{r})$ and $k_l(\mathbf{r})$ are determined. They define the local $P(\tau)$. After this each dislocation is displaced by a random value generated according to the local stress distribution function $P(\tau)$. The last two steps are repeated for each updating.

With this stochastic algorithm an initially homogeneous system of 2^{20} parallel straight edge dislocations with Burgers vectors of equal magnitudes in a double-slip configuration (with $\alpha = 1$) was investigated under constant external stress. (The slip geometry is defined according to Fig. 1.) To reduce finite size and surface effects the usual periodic replica technique [23,24] (with 224 replica dislocations) and periodic boundary conditions were used. The simulation area was divided into cells by 128×128 grid points.

After 5×10^5 updating the cell-like structure presented in Fig. 2 was obtained. Each cell wall predominantly consists of dislocations belonging to the same slip system and aligned in the other slip direction. This is in agreement with the prediction of the stability analysis presented above, namely, that periodic perturbations propagating in the direction perpendicular to the slip directions are preferred. An important feature of the obtained network is that characteristic cell size cannot be defined. In order to study the structure of the dislocation pattern developed, the standard box counting method was applied. According to Fig. 3 within the attainable magnification range (about a factor of 20) the number of nonempty boxes N versus box dimension relation can be well described by a power function with exponent $D \approx 1.86$, indicating fractal structure with dimension D. This is consistent with the results of Hähner *et al.* [26].

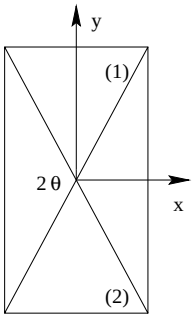

FIG. 1. The coordinate system used in the simulation. The glide planes of different type were chosen parallel to the diagonals ($\theta = \pm 60°$ to the x direction). The external stress had only $\sigma_{xx} \neq 0$.

In conclusion, a self-consistent field and a stochastic dislocation dynamics model was presented for 2D multiple-slip dislocation configuration. They represent the generalization of the corresponding single-slip models published earlier. It was pointed out that, beside the long range nature, the strong anisotropy of dislocation-dislocation interaction plays an important role in the

FIG. 2. Cell structure (left box) obtained from an initially homogeneous dislocation distribution after 5×10^6 updating. The dots represent dislocation lines orthogonal to the plane. The right-hand box shows the k map. The black and white lines are polarized dislocation walls containing dislocations with the same type of Burgers vector. It was found that the concentration of dislocations with opposite Burgers vectors in the polarized walls is less than 2%.

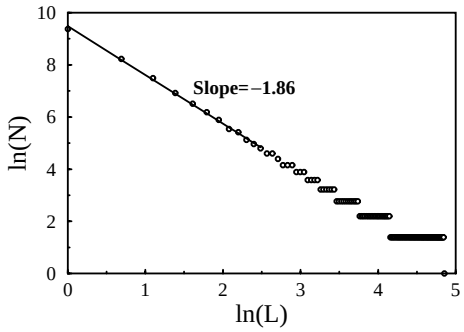

FIG. 3. Box counting analysis [the logarithm of the number of nonempty boxes $\ln(N)$ versus the logarithm of the box size $\ln(L)$] of the Fig. 2 cell structure. The simulation area was divided in 128×128 boxes. Each box containing less than 3 dislocations was considered empty during the box counting.

development of dislocation patterning, at least in the investigated 2D case. As it was indicated earlier by discrete dislocation dynamics simulation [10,14–16] if dislocation motion is allowed in more than one slip system, cell-like structure can form due to only the elastic dislocation-dislocation interaction, i.e., because of the internal elastic interaction the dislocation gas collapses into walls under the influence of the external stress. In contrast with this, in single-slip orientation dislocation multiplication needs to be introduced to obtain ordered dislocation structures [24]. One can state that even if dislocations are produced homogeneously by different multiplication processes the elastic dislocation-dislocation interaction leads to patterning. It is important to stress that, since the linear stability analysis does not predict growing perturbations, only the existence of stable ones, the observed cell formation is clearly due to nonlinear effects already in the early stage. The understanding of the influence of dislocation annihilation and multiplication requires further investigations.

Furthermore, the proposed stochastic approach made possible to increase considerably (by about a factor of 10^3) the affordable number of dislocations used in the simulations presented in the paper allowing us to analyze the dislocation pattern in more detail than earlier. Finally, it is necessary to note that the above 2D approach is only the first step toward learning how to deal with the strongly interacting dislocation assembly, but investigations are under way to extend it to 3D.

The authors are grateful to Professor J. Lenvai for stimulating discussions. The financial support of OTKA under Contract No. T 030791 is also acknowledged.

[1] M. N. Bassim, W. A. Jesser, D. Kuhlmann-Wilsdorf, and H. G. F. Wilsdorf, Mater. Sci. Eng. **81**, 122 (1986).
[2] D. L. Holt, J. Appl. Phys. **41**, 3179 (1970).
[3] J. M. Rickman and J. Viñals, Philos. Mag. A **75**, 1251 (1997).
[4] D. Walgraef and E. C. Aifantis, J. Appl. Phys. **15**, 688 (1985).
[5] J. Kratochvil and M. Saxlova, Scr. Metall. Mater. **26**, 113 (1993).
[6] A. Franek, R. Kalus, and J. Kratochvil, Philos. Mag. A **64**, 497 (1991).
[7] P. Hähner, Acta Mater. **44**, 2345 (1996).
[8] J. Lepinoux and L. P. Kubin, Scr. Metall. Mater. **21**, 833 (1987).
[9] A. N. Gullouglu, D. Srolovitz, R. LeSar, and P. Lomdahl, Scr. Metall. **23**, 1347 (1998).
[10] A. N. Gullouglu and C. S. Hartly, Model. Simul. Mater. Sci. Eng. **1**, 383 (1993).
[11] R. J. Amodeo and N. M. Ghoniem, Phys. Rev. B **41**, 6968 (1990).
[12] H. H. M. Cleveringa, E. Van der Giessen, and A. Needleman, Acta Mater. **45**, 3163 (1997).
[13] I. Groma and G. S. Pawley, Philos. Mag. A **67**, 1459 (1993).
[14] I. Groma and G. S. Pawley, Mater. Sci. Eng. A **164**, 306 (1993).
[15] R. Fournet and J. M. Salazar, Phys. Rev. B **53**, 6283 (1996).
[16] H. Y. Wang, R. LeSar, and J. M. Rickman, Philos. Mag. A **78**, 1195 (1998).
[17] D. B. Barts and A. E. Carlsson, Phys. Rev. E **52**, 3195 (1995).
[18] B. Devincre and M. Condat, Acta Metall. Mater. **40**, 2629 (1992).
[19] M. C. Fivel, T. J. Gosling, and G. R. Canova, Model. Simul. Mater. Sci. Eng. **4**, 581 (1996).
[20] I. Groma, Phys. Rev. B **52**, 9125 (1995).
[21] I. Groma, Phys. Rev. B **56**, 5807 (1997).
[22] I. Groma and P. Balogh, Acta Mater. (to be published).
[23] B. Bakó and I. Groma, Model. Simul. Mater. Sci. Eng. **7**, 181 (1999).
[24] B. Bakó and I. Groma, Phys. Rev. B **60**, 122 (1999).
[25] I. Groma and B. Bakó, Phys. Rev. B **58**, 2969 (1998).
[26] P. Hähner, K. Bay, and M. Zaiser, Phys. Rev. Lett. **81**, 2470 (1998).